Observation Error Statistics for *NOAA-10* Temperature and Height Retrievals

JERRY SULLIVAN

NOAA/NESDIS, Satellite Research Laboratory, Washington, D.C.

LEV GANDIN

Development Division, National Meteorological Center, Washington, D.C.

ARNOLD GRUBER

NOAA/NESDIS, Satellite Research Laboratory, Washington, D.C.

WAYMAN BAKER

Development Division, National Meteorological Center, Washington, D.C.

(Manuscript received 14 April 1992, in final form 17 February 1993)

ABSTRACT

In 1988, the algorithm for retrieving temperature soundings from radiances measured by NOAA's polar-orbiting satellites was changed from a statistical to a "physical" retrieval system. Because of this change, the National Meteorological Center (NMC) wanted to update the satellite temperature error statistics used in the NMC analyses. The authors, therefore, updated the estimates of observational error variances, horizontal covariances, and vertical correlations for layer mean temperatures retrieved from *NOAA-10* satellite radiance data. The temperature error statistics have also been used to estimate analogous error statistics for isobaric height.

The computations used radiosonde data as a substitute for true temperatures. Each "matchup" in the dataset consisted of a satellite retrieval close in space and time to a radiosonde sounding. The matchups were stratified into clear, partly cloudy, and cloudy cases, depending on the amount of cloud contamination in the satellite radiance data. In each of the nine mandatory pressure layers considered, from 1000–850 to 150–100 mb, the clear and partly cloudy matchup cases have nearly equal temperature error variances, while the variances for cloudy cases are substantially larger. Vertical error correlations for all three stratifications are similar. Root-mean-square height errors computed from satellite temperature errors are comparable to those computed from radiosonde errors in the clear and partly cloudy matchup cases, but larger in cloudy cases.

1. Introduction

Satellite temperature retrieval information, also called indirect sounding data, became available more than two decades ago, soon after the meteorological satellites were equipped with spectral radiometers measuring radiances (fluxes of outgoing radiation in various wavelength intervals). According to the radiative transfer theory, each radiance is strongly connected with the temperature profile in some layer of the atmosphere. This implies that the retrieval procedure may be based on a solution of the inverse problem of the atmospheric radiation theory.

There was much enthusiasm at that time among specialists in numerical weather prediction (NWP) about this new source of information, because data from each satellite can be used to produce a large number of retrieved temperature profiles, and particularly because such profiles may be obtained and used over vast areas poorly covered by direct (rawinsonde) sounding data, such as the oceans.

There was considerable effort in attempting to use the retrieval data in the same form as the rawinsonde data, that is, as a set of mandatory level rawinsonde heights. To achieve this, the retrieval data had to be "anchored" to an independently known height of some isobaric surface. This approach was used for a long time at the National Meteorological Center (NMC), as well as at some other centers, and it is still in use in the NMC regional data assimilation system (RDAS).

However, it was soon realized that a retrieval procedure, based on the inverse problem of the theory of radiative exchange, leads to an ill-posed mathematical problem, which reflects the fact that the same set of radiances may result from different temperature profiles. The solution of such a problem can also lead to computational instability. The original physical re-

Corresponding author address: Dr. Jerry Sullivan, Satellite Research Laboratory, NOAA/NESDIS, Washington, DC 20233.

trieval procedure was therefore replaced by a statistical retrieval procedure in 1979. The statistical procedure selected a mean temperature–radiance profile and then modified the temperature profile using empirically determined and periodically updated relationships between deviations from the mean radiance and deviations from the mean temperature. Such statistical retrievals were produced operationally by the National Environmental Satellite, Data, and Information Service (NESDIS) for many years. The statistically retrieved temperature profiles (transformed to isobaric thickness profiles) were disseminated as satellite temperature (SATEM) reports and used by data assimilation systems at NMC, the European Centre for Medium-Range Weather Forecasts (ECMWF), and several other forecast centers. The procedure to assimilate these data was, and continues to be, different at different centers. The NMC RDAS assimilates anchored heights, while ECMWF includes the direct application of SATEM thicknesses, using the cross correlation between thicknesses and heights.

In an attempt to improve the quality of satellite temperature retrievals, the purely statistical methodology was replaced in 1988 by a "physical" retrieval scheme (Dey et al. 1989; Fleming et al. 1986). The procedure, developed and implemented by NESDIS, consists of two steps: 1) a library search, resulting in a first approximation to the temperature profile; and 2) the solution of physical equations applied to deviations from this first guess. There are indications that the transition from statistical to physical retrievals has resulted in some improvement of the quality of retrieved temperature profiles. A more recent retrieval technique (not addressed in this paper) that uses a model 6-h forecast as the first guess has also generated encouraging preliminary results.

The data assimilation systems at major forecast centers have also undergone several improvements. The spectral statistical interpolation (SSI) method replaced the gridpoint optimum interpolation scheme in the NMC global data assimilation system (GDAS). Temperatures, including retrieved ones, are directly assimilated using the SSI scheme, which excludes one source of error: those originating in the course of height anchoring. Retrieved mean temperature of thick layers is used in the ECMWF data assimilation system instead of retrieved temperature for each mandatory layer in order to diminish the influence of retrieval errors on the assimilated height fields.

However, the improvement of both retrievals and data assimilation systems did not lead to any substantial improvement of analyses and forecasts over regions with a high or intermediate density of the rawinsonde network. A partial cause of the low impact of retrievals on analyses and forecasts is their indirect nature, the fact that radiances are measured rather than temperatures. Because of this, relationships between radiances and temperatures used in the retrieval process are valid only on the average, not for a retrieval at every particular location and time.

This leads to a new feature not found in radiosonde data; the fact that retrieval errors are correlated in space. Systematic errors in the cloud clearing and water vapor algorithms in the retrieval process could also account for this feature. The large cross-track scan velocity (350 km s^{-1}) and orbital velocity (7 km s^{-1}) of the satellite lead to another possible explanation for the spatial correlation of errors; a bias that persists for a relatively short time could lead to a bias over relatively large distances.

Whatever its cause, the fact that random errors in satellite retrieval data are horizontally correlated has been verified experimentally by several investigators. Particularly, retrieval error statistics have been computed by Schlatter and Branstator (1979), Schlatter (1981), and Watkins and Gruber (1987). Furthermore, the influence of this random error correlation on the informational value of such data and on the data assimilation problem has been examined in several studies (i.e., Gandin et al. 1972; Gandin and Kagan 1974; Bergman and Bonner 1976).

Horizontally correlated random errors behave, to some extent, like systematic errors (also called biases); they are often of the same sign and close to each other in absolute value over comparatively large areas. There is, however, a substantial difference between the two: while averaging over a sample does not significantly change a systematic error, the mean value of a random error, whether spatially correlated or not, is practically zero over a large sample. In other words, although the pattern of random horizontally correlated errors in each particular case is analogous to that of a bias, the values of correlated errors and their sign vary from one case to another, and that is what makes their averaged values tend to zero.

The correlation between random observational errors can and should be taken into account in the data assimilation system. Consider, for simplicity, two-dimensional univariate optimum interpolation from N observation points onto a grid point:

$$\hat{f}_0 = \sum_{i=1}^{N} w_i f_i, \tag{1}$$

where f is the deviation of some parameter, for example, temperature, from its background field, f_0 is the interpolated value of this deviation at the grid point, f_i ($i = 1, 2, \cdots, N$) are its observed values, and w_i ($i = 1, 2, \cdots, N$) are interpolation weights computed from the system of N linear equations

$$\sum_{j=1}^{N} (\mu_{ij} + \gamma_i \gamma_j \nu_{ij}) w_j = \mu_{0i}. \tag{2}$$

Here, $\mu(r)$ is the correlation function of true values of f, $\nu(r)$ is the correlation function of observation (or retrieval) errors, μ_{ij} and ν_{ij} are values of these functions, corresponding to the distance r_{ij} between points i and

j, and γ_j is the relative variance of observation or retrieval error at point j (i.e., the ratio of the error variance to the variance of actual deviations f).

Rawinsonde observation errors are not correlated horizontally:

$$\nu_{ij} = \begin{cases} 0, & j \neq i \\ 1, & j = i. \end{cases}$$

Therefore, if all N observations in (1) come from rawinsondes, then the system (2) may be rewritten as

$$\sum_{j=1}^{N} \mu_{ij} w_j + \gamma_i^2 w_i = \mu_{0i}, \qquad (3)$$

and differs from the system for interpolating exact values only by increasing diagonal elements of the system matrix. On the other hand, the comparison between (2) and (3) shows that the (positive) correlation between retrieval errors leads to an increase in off-diagonal elements of the matrix. It can be shown that this results, with other conditions equal, in diminishing the weights w_i.

It is easy to write down the system of equations for a more general case, when there are both rawinsonde and satellite data available. For example, if there are rawinsonde data at points 1 and 2 and retrieval data at points 3–5, then the system (2) is

$$\begin{aligned}
(1 + \gamma_r^2) w_1 + \mu_{12} w_2 + \mu_{13} w_3 + \mu_{14} w_4 + \mu_{15} w_5 &= \mu_{01} \\
\mu_{12} w_1 + (1 + \gamma_r^2) w_2 + \mu_{23} w_3 + \mu_{24} w_4 + \mu_{25} w_5 &= \mu_{02} \\
\mu_{13} w_1 + \mu_{23} w_2 + (1 + \gamma_s^2) w_3 + (\mu_{34} + \gamma_s^2 \nu_{34}) w_4 + (\mu_{35} + \gamma_s^2 \nu_{35}) w_5 &= \mu_{03} \\
\mu_{14} w_1 + \mu_{24} w_2 + (\mu_{34} + \gamma_s^2 \nu_{34}) w_3 + (1 + \gamma_s^2) w_4 + (\mu_{45} + \gamma_s^2 \nu_{45}) w_5 &= \mu_{04} \\
(\mu_{15} w_1 + \mu_{25} w_2 + (\mu_{35} + \gamma_s^2 \nu_{35}) w_3 + (\mu_{45} + \gamma_s^2 \nu_{45}) w_4 + (1 + \gamma_s^2) w_5 &= \mu_{05}. \qquad (4)
\end{aligned}$$

These examples demonstrate that in order to properly assimilate the satellite retrieval data it is important to know the correlation function for errors in these data. To compute such functions is not an easy task. Collocation with rawinsonde observations, which is considered as the best way for such investigations, can be achieved only approximately, both in space and in time. The error correlation functions, as well as their variances, should not be the same under various cloudiness conditions and should be, therefore, determined separately for different gradations of cloudiness. Moreover, it is necessary to also have the cross-correlation functions for errors under different degrees of cloudiness in order to assimilate such data at every point. The asynoptic nature of satellite retrieval data prevents the averaging in time for the same pair of points. The averaging of individual products over some distance intervals (also called "bins") can be performed instead. One also has to take into account the fact that both the retrieval methods and the satellites may change, and the error correlation functions, computed with data from a particular satellite and with a particular retrieval procedure are not necessarily valid for another satellite and/or retrieval method. In other words, the information about the retrieval error correlation functions should be updated every time when a new satellite with a different instrument has been launched, or the temperature retrieval method has been modified.

In this paper, we estimate the error variance and model the covariance as a function of distance between locations for the layer mean temperature (hereafter referred to as temperature) retrieved from satellite radiances. The temperature retrievals were obtained from the *NOAA-10* polar orbiter.

Many data assimilation systems, such as the NMC RDAS (DiMego 1988), produce analyses in terms of isobaric heights rather than temperatures. Satellite temperatures can be accounted for within such systems by using the hydrostatic equation to compute the corresponding height profile from each satellite temperature profile. This enables the use of temperature retrieval error statistics to estimate corresponding statistics for isobaric heights.

The next section contains a description of the satellite and radiosonde temperature data sources. Then, results for the temperature error variance, horizontal covariance, and vertical correlation are discussed. A section on the accuracy of fitting the horizontal covariance data by an analytic function is also included. Finally, the statistical results, variance, horizontal correlation, and vertical correlation are considered for isobaric height errors.

2. Data sources

We used data from one satellite, the *NOAA-10,* and from more than 18 000 radiosondes. The *NOAA-10* satellite orbits approximately 850 km above the earth, completing one orbit in 102 min or slightly more than 14 orbits per day. The availability of satellite–radiosonde matchups is determined mainly by radiosonde locations and launch times. Radiosonde stations are predominantly located on Northern Hemisphere land areas, and take observations twice daily at 0000 and 1200 UTC. The *NOAA-10* satellite passes over most locations twice a day, at approximately 0730 and 1930 LST. In our matchups, the satellite overpass time was required to be within 4 h of the radiosonde launch, and the distance between radiosonde station and the

center of the satellite footprint had to be less than 330 km. (Most were much closer.) The time constraint eliminated most locations in Africa and Europe. Consequently, most matchups in our dataset were from Asia and North America, with a relative few from South America and Australia. Figure 1 shows a map with locations of radiosonde stations that contributed to the matchup sample. It also indicates qualitatively how many matchups are at each location.

As a substitute for "true" ambient temperature, we used the temperature measured by radiosondes. The computed statistics actually refer to the "difference" between satellite and radiosonde temperature, but we use this difference as the satellite observational error. Using radiosonde measurements as a replacement for the true temperature introduces the radiosonde observational error into our calculation. Other errors arise because the collocations are imperfect and because the 3-week time period is not a fully representative sample of the range of satellite temperature errors.

For temperature retrievals up to 100 mb, data were collected by two radiometers, the High-Resolution Infrared Radiation Sounder (HIRS) and the Microwave Sounding Unit (MSU). More details about the radiometers can be found in Smith et al. (1979). The HIRS radiometer has better resolution in both the vertical and horizontal but has the disadvantage that clouds can contaminate measurements in the infrared channels. Because of the cloud problem, there are three retrieval types (McMillin and Dean 1982): clear, partly cloudy, and cloudy. (In areas that are partly clear and partly cloudy, the partly cloudy algorithm attempts to extract radiances for the clear areas only.) The clear and partly cloudy algorithms rely mainly on data from the HIRS instrument, while cloudy retrievals use mostly microwave channel data. We stratified the satellite temperature observational errors by examining the three retrieval types separately.

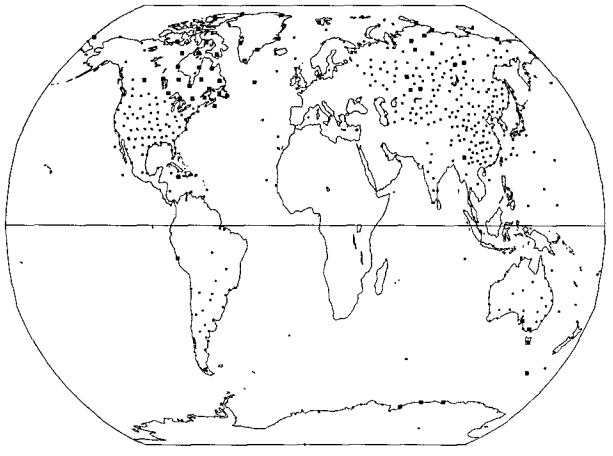

FIG. 1. Matchup radiosonde station locations. The larger boxes denote locations with more than 50 matchups, and the small squares locations with from 15 to 50 matchups.

The satellite–radiosonde matchups are from the period 14 April to 7 May 1989. This large dataset contained roughly 9000 clear matchups, 4500 cloudy matchups, and 4500 partly cloudy matchups. The distance between soundings in a matchup is usually less than 300 km, while the time difference is usually less than 3 h. For example, in the clear matchup case, 40% of the satellite soundings in a matchup were taken within an hour of their radiosonde counterpart, and the mode of the distances between the satellite and radiosonde soundings was 125 km.

3. Temperature error variance

If $T_{S,n}$ and $T_{R,n}$ are the satellite and radiosonde temperatures in a given layer for matchup n, then we denote the satellite temperature error by

$$t_n = T_{S,n} - T_{R,n}. \tag{5}$$

The mean and variance of the error, taken over the N matchups in the ensemble, are defined by

$$\bar{t} = \sum_{n=1}^{N} \frac{t_n}{N}, \tag{6}$$

and

$$\sigma^2(t) = \sum_{n=1}^{N} \frac{(t_n - \bar{t})^2}{N} = \overline{(t - \bar{t})^2}. \tag{7}$$

The mean and variance were calculated for nine layers in the vertical, the layers bounded by pressure surfaces at 1000, 850, 700, 500, 400, 300, 250, 200, 150, and 100 mb. Equation (7) can be rewritten as

$$\sigma^2(t) = \overline{t^2} - (\bar{t})^2. \tag{8}$$

The two quantities on the right-hand side of Eq. (8) are graphed in Fig. 2. The last term in Eq. (8) is small compared to the total variance. Cloudy matchups have the largest variance, while the clear and partly cloudy cases have values fairly close to each other, except for the surface layer. This feature has also been found by Watkins and Gruber (1987). It is plausible since temperatures in cloudy cases are retrieved mainly from the MSU radiometer, which has poorer vertical and horizontal resolution than the HIRS infrared radiometer used in the other cases. The surface layer has the largest variance. This layer is well known to be the least accurate for satellite temperature soundings.

The temperature error variance increases in the layer from 300 to 200 mb. It appears that the larger variance in this layer results from the fact that satellite retrievals have coarser vertical resolution than radiosonde measurements do. They do not resolve nonlinear temperature profiles, particularly inversions, as well as radiosondes, and as a consequence, the variance is large in layers with temperature inversions. Our dataset is dominated by matchups from the Northern Hemi-

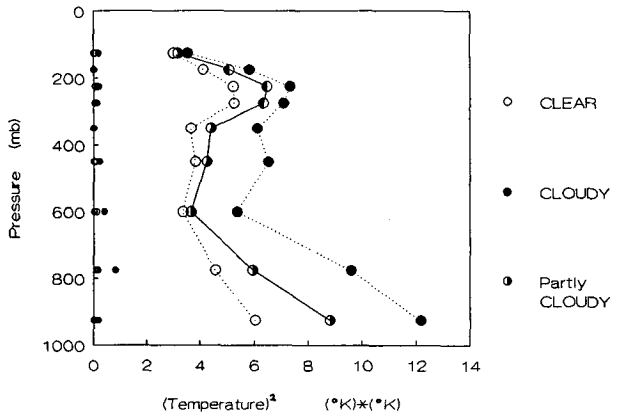

FIG. 2. Temperature error variance components for clear, cloudy, and partly cloudy matchup cases. The large symbols denote the $\overline{t^2}$ component, and the small symbols (which cluster around zero) represent the $(\bar{t})^2$ part.

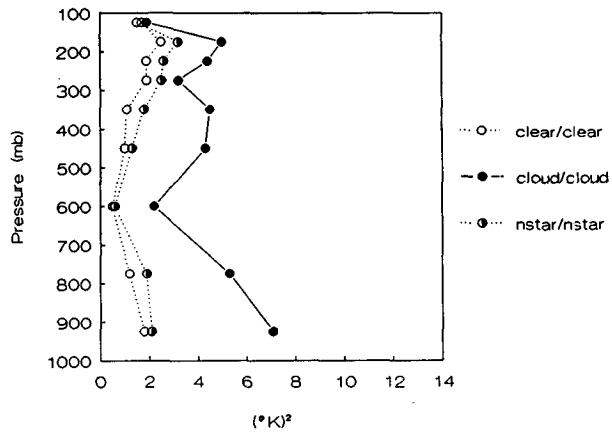

FIG. 3. Estimates for the temperature error variance C_0. (Nstar is a technical name for partly cloudy.)

sphere midlatitudes where inversions routinely occur in the 300–200-mb layer (and near the surface).

4. Horizontal covariance of temperature errors

For each layer, the horizontal covariance of satellite temperature errors between locations 1 and 2 in the layer is estimated by computing

$$m(t_1, t_2) = \overline{(t - \bar{t})_1 (t - \bar{t})_2} = \overline{t_1 t_2} - \bar{t}_1 \bar{t}_2. \quad (9)$$

We assume that the horizontal covariance is a function of *only* the separation distance between two locations in a pressure layer. The literature contains a variety of functions that reasonably describe the covariance data. We chose a function that was introduced by Yudin (1950) and used by Thiebaux (1977):

$$C(r) = C_0\left(1 + \frac{r}{L}\right)\exp\left(\frac{-r}{L}\right), \quad (10)$$

where r is the distance between two locations, $C(r)$ is the covariance function, C_0 is its value at $r = 0$, and L is a length-scale factor. The parameters C_0 and L were found by fitting the analytic function to the covariance values using a weighted least-squares method. The weight in each distance bin is proportional to the number of temperature products in the bin.

To compare measurements that were close together in time, we required that the satellite temperature soundings in a matchup pair were within 7 min of each other. Since the satellite orbital velocity is more than 400 km min^{-1}, this allows up to a 2800-km separation distance between matchup pairs. The satellite–satellite distance between each matchup pair was calculated and the temperature error products put into distance bins. Each distance bin is 100 km wide; the first bin is from 150 to 250 km, and the last from 1950 to 2050 km. (The final results are practically independent of bin width.) The covariance in a distance bin is computed by averaging the individual temperature error products in the bin. Table 1 shows the number of temperature error products in each distance bin, averaged over the nine vertical layers. Typically, the surface layer contains only about 30% as many products as the average.

Figure 3 shows the parameter C_0 plotted as a function of pressure layer. For all matchup cases, the shapes of the C_0 versus pressure curves are very similar to the shapes of the variance curves shown in Fig. 2. The main difference is that for each matchup case C_0 is less than the variance. The variation of the length scale L as a function of pressure layer is shown in Fig. 4. The length scale values are generally largest for the clear–clear matchup case, in contrast to the C_0 behavior. Values cluster in the 400–500-km range.

5. Accuracy of the horizontal covariance fit

This section shows graphically and numerically to what extent the analytic functions fit the data in each layer. Figure 5 shows the fits for both clear–clear and partly cloudy–partly cloudy matchup cases. For the clear–clear case, the analytic functions fit the data quite

TABLE 1. Average number of temperature error products in every second distance bin for each matchup–matchup case.

Distance (km)	200	400	600	800	1000	1200	1400	1600	1800
clear–clear	729	2299	3119	3165	3316	3414	3171	2558	2258
cloudy–cloudy	274	836	1022	991	998	1029	960	786	713
partly cloudy–partly cloudy	201	679	859	959	879	965	864	681	637

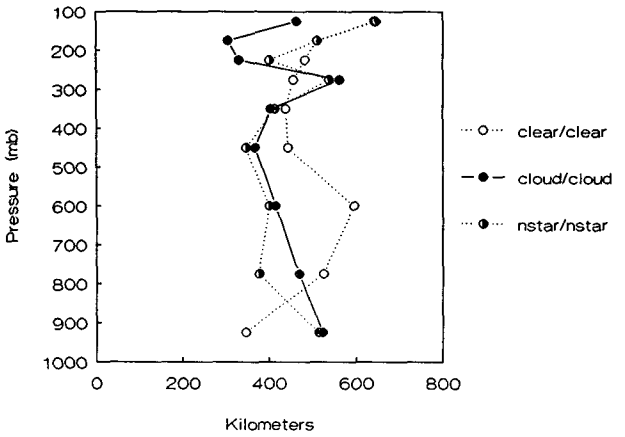

FIG. 4. Estimates for the length scale L. (Nstar is a technical name for partly cloudy.)

well, with the poorest fit occurring in the surface layer. The fits for the cloudy–cloudy matchup case are also good. However, as Fig. 5 shows, the covariance data for the first three layers of the partly cloudy–partly cloudy case are very erratic. The largest discrepancy in each fit typically occurs at the closest distance bins. The data may be in error here, since there are relatively few data points in these bins. However, the fit is weighted by the number of points in a bin, so data in distance bins farther from the origin influence the fit more.

For the usual type of fit, the quantity

$$100\left\{\frac{\sum_{n=1}^{v} w_n[C_n - C(r_n)]^2}{\sum_{n=1}^{v} w_n(C_n - C)^2}\right\}, \qquad (11)$$

where C_n is the covariance value at separation distance r_n, $C(r_n)$ is the fitted value, and C is the mean covariance, shows the percent of variance around the mean still unexplained by the fit. The weights w_n are proportional to the number of temperature error products in the nth distance bin, and v is the number of bins. The usual meaning given to the statistic, percent of unexplained variance, is valid only when the coefficients in the fit are linear. In Eq. (10), the coefficient L occurs nonlinearly in the term $\exp(-r/L)$. However, the "unexplained variance" statistic defined in Eq. (11) is still helpful for comparison purposes. It ranges from 0 to 100 for our function, and low values indicate a good fit.

Table 2 shows the quantity for all matchup–matchup cases. [If C_0 and L were linear in Eq. (10), the single-digit numbers would imply a 0.95 correlation between the fit and the covariance data.] The values quantify what Fig. 5 shows: excellent fits above the surface layer and moderate to good fits in the surface layer. The fit for the partly cloudy–partly cloudy matchups is much

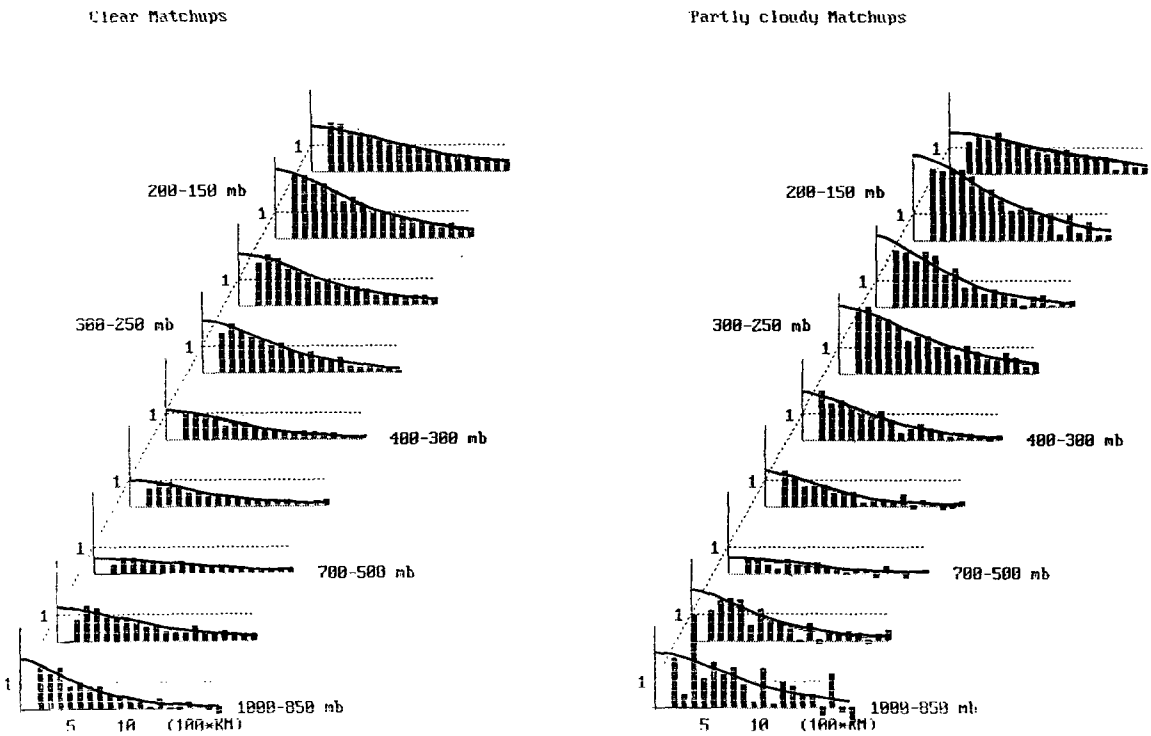

FIG. 5. The fit of the analytic temperature error covariance curves to the histogram data for the clear–clear and partly cloudy–partly cloudy matchup cases.

TABLE 2. Values for different matchup–matchup types of the "percent of variance around the mean" still unexplained by the analytic covariance function fit.

Pressure layer (mb)	clear / clear	cloudy / cloudy	partly cloudy / partly cloudy
	Satellite–Radiosonde		
150–100	3	16	13
200–150	2	3	8
250–200	4	4	10
300–250	5	6	8
400–300	7	7	9
500–400	9	5	17
700–500	14	7	47
850–700	17	11	27
1000–850	11	16	62

poorer than for the other matchup–matchup types in the first three layers.

6. Vertical correlation of temperature errors

The vertical correlation between temperature errors from layers j and k is estimated by

$$r(t_j, t_k) = \frac{m(t_j, t_k)}{\sigma(t_j)\sigma(t_k)}. \qquad (12)$$

These correlations are shown in Table 3 for the clear matchup cases. The nearest off-diagonal coefficients are positive and high. The correlations then fall off rapidly as the distance between layers increases, and in some cases fall to a moderately large negative value. These same features are also found for cloudy and partly cloudy matchup cases.

7. Isobaric height error variance

There are different ways to take satellite temperature retrieval data into account within data assimilation systems that produce their analyses in terms of height rather than layer mean temperature. The simplest way is to use the hydrostatic equation to compute the corresponding height profile from each satellite temperature profile. An independently determined height of some reference isobaric surface is used to anchor the height profile. This way has been used for many years in the NMC data assimilation systems, for example, to assimilate retrieval data over the oceans, with the 1000-mb height field applied as the anchor.

The height at any mandatory pressure level L, H_L, is the sum of the thicknesses of all the intermediate layers:

$$H_L = Z_0 + \sum_{k=1}^{L} Z_k = Z_0 + \sum_{k=1}^{L} a_k T_k, \qquad (13)$$

where Z_0 is the height of the 1000-mb surface, Z_k is the thickness of layer k, and T_k is the layer mean temperature. The coefficients a_k are obtained from integrating the hydrostatic equation

$$a_k = \frac{R}{g} \ln\left(\frac{p_{k-1}}{p_k}\right),$$

with R the gas constant for dry air, g the acceleration of gravity, and p_k the mandatory-level pressure. This set of coefficients depends only on the mandatory pressure levels.

The height error, the difference between heights computed from satellite and radiosonde temperatures, is defined as

$$h_L = (Z_S - Z_R)_0 + \sum_{k=1}^{L} a_k (T_S - T_R)_k. \qquad (14)$$

Using the notation defined in Eqs. (5) and (6), we can write the deviation from the mean as

$$(h - \bar{h})_L = (z - \bar{z})_0 + \sum_{k=1}^{L} a_k (t - \bar{t})_k. \qquad (15)$$

To compute the variance of height errors, we assume that the error in the anchor height is uncorrelated with temperature errors in any layer because the anchor height is obtained from an independent source, that is,

$$\overline{(z - \bar{z})_0 (t - \bar{t})_k} = 0$$

TABLE 3. Vertical correlations of satellite–radiosonde layer mean temperature errors for clear matchup cases. (Correlations are expressed in percent.)

Pressure layer (mb)	1000–850	850–700	700–500	500–400	400–300	300–250	250–200	200–150	150–100
150–100	−4	−5	−5	−8	−12	−4	13	54	100
200–150	−3	−6	−14	−22	−23	−2	51	100	
250–200	1	−5	−25	−29	−6	57	100		
300–250	5	−5	−20	−10	47	100			
400–300	6	7	20	58	100				
500–400	7	24	68	100					
700–500	9	53	100						
850–700	40	100							
1000–850	100								

for any layer k. With this assumption, the height error variance $\sigma^2(h_L)$ at pressure level L is

$$\sigma^2(h_L) = \sigma^2(Z_0) + \sum_{j=1}^{L}\sum_{k=1}^{L} a_j a_k \overline{(t-\bar{t})_j(t-\bar{t})_k}. \quad (16)$$

The averaged term in the double sum is the vertical covariance of temperature errors between layers j and k. To estimate this, we use the vertical temperature error correlations [Eq. (12)] and denote the variances in layers j and k as $C_{0,j}$ and $C_{0,k}$, following the notation of Eq. (10). Using this definition, Eq. (16) can be written as

$$\sigma^2(h_L) = \sigma^2(Z_0) + \sum_{j=1}^{L}\sum_{k=1}^{L} a_j a_k (C_{0,j}C_{0,k})^{0.5} r(t_j, t_k). \quad (17)$$

The right-hand side of Eq. (17) contains only temperature error variances and the vertical correlations between errors in separate layers.

Typical results for the rms height error computation using Eq. (17) are presented in Figs. 6 and 7. In these calculations, we set $\sigma^2(z_0) = 100\ \text{m}^2$. To provide some information on our confidence in these values, we also estimated the rms error of these computations. These estimates are obtained by the equation

$$(\sigma_{\text{col}})_L^2 = \sum_{k=1}^{L} a_k^2[\sigma^2(t_k) - C_{0,k}], \quad (18)$$

where the variances in brackets express the joint influence of collocation errors and of random errors in information used for collocation, that is, in the radiosonde data. Unlike Eq. (17), Eq. (18) does not account for any vertical correlation between the errors. One can speculate that some positive vertical correlation should exist between the collocation errors in temperature, but nothing is known about this kind of correlation, and it would be very difficult, if not impossible, to estimate it. Equation (18) gives a lower limit for the rms collocation errors; the actual errors can only be larger. We also examined the influence of vertical temperature error correlations on the height error variances by setting $r(t_j, t_k) = 0$ in Eq. (17) when j and k are different. The results, also presented in Figs. 6 and 7, demonstrate that including the vertical correlation of temperature errors leads to a marked increase in rms height errors.

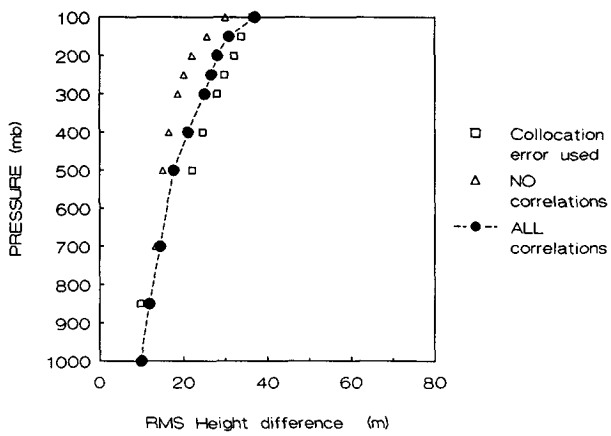

FIG. 6. Root-mean-square height errors computed using three different assumptions about vertical correlations between layer mean temperature errors, for clear–clear matchups.

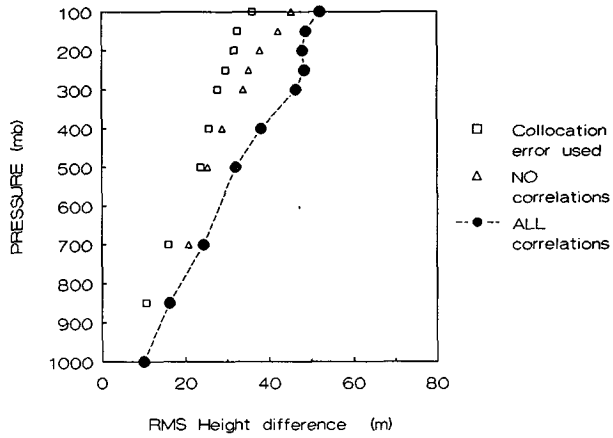

FIG. 7. Root-mean-square height errors computed using three different assumptions about vertical correlations between layer mean temperature errors, for cloudy–cloudy matchups.

Our results show that the random collocation errors are of the same order of magnitude as the random observational errors themselves. Collocation errors play a smaller role for cloudy retrievals, not because they are smaller—the opposite is true—but because the observational errors are substantially larger under cloudy conditions. The general conclusion is that the accuracy of our results should not be overestimated, and only the distinct regularities demonstrated in these results can be trusted, not small differences.

Generally, the rms height errors presented in Figs. 6 and 7 do not differ substantially from those found in previous investigations. Despite the improvements in the instrumentation, as well as in retrieval procedures, these errors remain large, about twice as large on the average, as the radiosonde observational errors.

We now compare our results on the horizontal correlation of the retrieval errors to some of those obtained and accounted for elsewhere. Watkins and Gruber (1987) also used a global dataset, comparing satellite retrievals with individual radiosonde soundings. They used the same analytical model for the correlation function as we did, Eq. (10). Schlatter (1981) compared retrievals with temperatures obtained from statistical objective analyses of radiosonde data over the United States and southern Canada. Schlatter and Branstator (1979) also compared retrievals to temperature analyses, using only European data. Both of these

studies modeled the correlation as a function of distance by the function $\exp(-kr^2)$.

The correlation functions calculated by Watkins and Gruber from global data decreased (slightly) faster with distance than ours for the clear case and more slowly for the cloudy case. To compare our results with the Schlatter study, we used a subset of our global dataset that contained data from the United States alone. As shown in Fig. 8, the Schlatter correlation curve decreases more rapidly than our United States curve. As to the Schlatter and Branstator results, their correlation function decreases much faster than any of the others, as also shown in Fig. 8.

We are not certain why the "new" values of the error correlation radii are higher than the "old" ones. The instruments, satellite radiometers and radiosonde thermistors, did not change considerably over the period. The satellite retrieval algorithm did, however, which is why we updated the error statistics. Another factor, perhaps the major one, is that the earlier work compared retrievals to temperature analyses and the later work compared them to individual radiosonde temperatures.

This high correlation, coupled with the high correlation of the actual temperature or height values themselves, results in the fact that each satellite observation contains little information in addition to that already contained in a neighboring observation. The closer this neighboring point is, the less additional information it contains. This strongly suggests that, in the course of the data assimilation, it is desirable to replace a group of neighboring satellite height observations by a single value rather than to use each datum separately.

It is necessary to stress, however, that while being a negative factor when analyzing the heights or temperatures themselves, the horizontal correlation of the observation errors is a positive factor when determining their differential characteristics, like the horizontal gradients. It is easy to show that the correlation of observational error leads, with other conditions equal, to an increase in the accuracy of differential characteristics derived from such data. To make full use of this advantage, it is desirable to slightly modify the assimilation procedure, namely, to compute gradients and/or other differential characteristics directly from observed data, avoiding any analysis of the height or temperature itself. We believe that this point deserves serious attention.

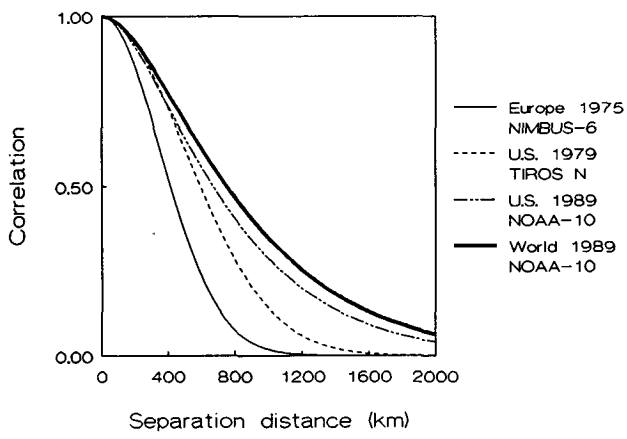

FIG. 8. Satellite horizontal temperature error correlations as a function of separation distance, for different satellites and different areal coverage.

TABLE 4. Vertical correlations of satellite–radiosonde height errors, assuming *no* vertical correlations between temperature errors in different layers, for clear matchup cases. (Correlations are expressed in percent.)

Pressure level (mb)	850	700	500	400	300	250	200	150
100	40	45	50	55	62	67	73	86
150	46	52	59	64	73	78	86	
200	54	61	69	75	85	91		
250	59	67	75	82	93			
300	64	72	81	88				
400	72	81	92					
500	79	89						
700	89							

8. Vertical correlation of height errors

The final statistics considered here are the vertical correlations of height retrieval errors. The vertical correlation of the satellite–radiosonde height errors between mandatory pressure levels L and M is defined as

$$r(h_L, h_M) = \frac{m(h_L, h_M)}{\sigma(h_L)\sigma(h_M)}. \tag{19}$$

This definition formally resembles the vertical correlation of temperature errors in Eq. (12) but there is an important difference.

If height H_L is greater than H_M, we have

$$H_L = H_M + \sum_{k=M+1}^{L} Z_k = H_M + \sum_{k=M+1}^{L} a_k T_k. \tag{20}$$

Equation (20) enables us to write Eq. (15) as

$$(h - \bar{h})_L = (h - \bar{h})_M + \sum_{k=M+1}^{L} a_k (t - \bar{t})_k. \tag{21}$$

When this relation is substituted into the numerator of the vertical height error correlation definition, we obtain

$$r(h_L, h_M) = \frac{\sigma^2(h_M) + \sum_{j=1}^{M} \sum_{k=M+1}^{L} a_j a_k (C_{0,j} C_{0,k})^{0.5} r(t_j, t_k)}{\sigma(h_L)\sigma(h_M)}, \tag{22}$$

TABLE 5. Vertical correlations of satellite–radiosonde height errors, using vertical correlations between temperature errors in all separate layers, for clear matchup cases. (Correlations are expressed in percent.)

Pressure level (mb)	850	700	500	400	300	250	200	150
100	37	45	48	49	54	61	73	91
150	46	55	60	63	69	78	90	
200	51	63	70	75	86	95		
250	53	67	78	86	96			
300	56	71	85	94				
400	65	82	96					
500	76	93						
700	91							

where the index j in the double sum ranges from 1 to M, and the index k from $M + 1$ to L. This equation connects the vertical height error correlation with the temperature error variances and vertical temperature error correlations.

Equation (22) shows that even when temperature retrieval errors in separate layers are uncorrelated, $r(t_j, t_k) = 0$, errors in heights computed from retrieved temperatures using the hydrostatic equation are still positively correlated because of the $\sigma^2(h_M)$ term. The same thicknesses that add up to the height H_M are also the first M thicknesses of height H_L. If $r(t_k, t_j) = 0$ in Eq. (22), then

$$r(h_L, h_M) = \frac{\sigma(h_M)}{\sigma(h_L)}. \qquad (23)$$

Values of the vertical correlation of height errors computed from Eqs. (22) and (23) are presented in Tables 4 and 5 for the clear matchup case. They show that the vertical correlation of height errors is much higher than the vertical correlation of temperature errors shown in Table 3, and depends only slightly on the latter. This means that data at different elevations contain very little additional information with respect to each other, analogous to the case with data at neighboring points in the horizontal. However, the vertical correlation of height errors, unlike the horizontal one, is characteristic not only of satellite retrieval data but also of radiosonde height data. As long as the height data are computed from radiosonde temperature measurements by means of the hydrostatic equation, the height errors will be strongly correlated in the vertical.

Acknowledgments. Tony Reale (NESDIS) and Andy Nappi (Hughes STX, Corporation) prepared the satellite–radiosonde matchup data. Jean Thiebaux (NMC) assisted with theoretical issues and provided a number of helpful suggestions on the manuscript. Larry McMillin (NESDIS) also thoroughly reviewed the paper. The encouragement and support of Eugenia Kalnay (NMC) is sincerely acknowledged. We wish to thank the referees for their aid with the logical structure of the paper, and also for many challenging questions.

REFERENCES

Bergman, K. H., and W. D. Bonner, 1976: Analysis error as a function of observation density for satellite temperature soundings with spatially correlated errors. *Mon. Wea. Rev.*, **104,** 1308–1316.

Dey, C. H., R. A. Petersen, B. A. Ballish, P. M. Chaplan, L. L. Morone, H. J. Thiebaux, G. H. White, H. E. Fleming, A. L. Reale, D. G. Gray, M. D. Goldberg, and J. M. Daniels, 1989: An evaluation of NESDIS TOVS retrievals using data impact studies. NOAA Tech. Memo., NWS NMC 69, 25 pp.

Fleming, H. E., M. D. Goldberg, and D. S. Crosby, 1986: Minimum variance simultaneous retrieval of temperature and water vapor from satellite radiance measurements. *Second Conf. on Satellite Meteorology/Remote Sensing and Applications,* Williamsburg, VA, Amer. Meteor. Soc., 20–23.

——, ——, and ——, 1988: Operational implementation of the minimum variance simultaneous method. *Third Conf. on Satellite Meteorology and Oceanography,* Anaheim, CA, Amer. Meteor. Soc., 16–19.

Gandin, L. S., and R. L. Kagan, 1974: Construction of a system for objective analysis of heterogenous data based on the method of optimum interpolation and optimum agreement. *Meteorol. Gidrol.,* **5,** 1–11.

——, R. L. Kagan, and L. I. Polishchuk, 1974: Information value estimates for various meteorological observing systems. *Tr. GGO,* **208,** 120–131.

Goldberg, M. D., J. M. Daniels, and H. E. Fleming, 1988: A method for obtaining an improved initial approximation for the temperature/moisture retrieval problem. *Third Conf. on Satellite Meteorology and Oceanography,* Anaheim, CA, Amer. Meteor. Soc., 20–23.

McMillin, L. M., 1991: Evaluation of a classification method for retrieving atmospheric temperatures from satellite measurements. *J. Appl. Meteor.,* **30,** 432–446.

——, and C. Dean, 1982: Evaluation of a new operational technique for producing clear radiances. *J. Appl. Meteor.,* **21,** 1005–1014.

Schlatter, T. W., 1981: An assessment of operational TIROS-N temperature retrievals over the United States. *Mon. Wea. Rev.,* **109,** 110–119.

——, and G. W. Branstator, 1979: Estimation of errors in *Nimbus* 6 profiles and their spatial correlation. *Mon. Wea. Rev.,* **107,** 1402–1413.

Smith, W. L., H. M. Woolf, C. M. Hayden, D. Q. Wark, and L. N. McMillin, 1979: The TIROS-N operational vertical sounder. *Bull. Amer. Meteor. Soc.,* **60,** 1177–1187.

Thiebaux, H. J., 1977: Extending estimation accuracy with anisotropic interpolation. *Mon. Wea. Rev.,* **105,** 691–699.

Watkins, C., and A. Gruber, 1987: Determination of the observational error of satellite retrievals. *Adv. Space Res.,* **7,** 343–346.

Yudin, M. I., 1950: Some problems in the theory of Meteorological fields. *Tr. GGO,* **81,** 3–18.